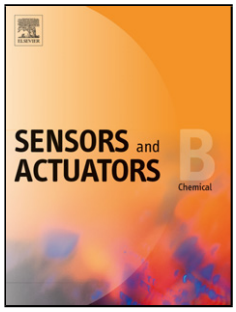

Title: Highly formaldehyde-sensitive, transition-metal doped ZnO nanorods prepared by plasma-enhanced chemical vapor deposition

Author: Peng Hu Ning Han Dangwen Zhang Johnny C. Ho Yunfa Chen

PII: S0925-4005(12)00298-5
DOI: doi:10.1016/j.snb.2012.03.035
Reference: SNB 13987

To appear in: *Sensors and Actuators B*

Received date: 28-11-2011
Revised date: 26-2-2012
Accepted date: 12-3-2012

Please cite this article as: P. Hu, N. Han, D. Zhang, J.C. Ho, Y. Chen, Highly formaldehyde-sensitive, transition-metal doped ZnO nanorods prepared by plasma-enhanced chemical vapor deposition, *Sensors and Actuators B: Chemical* (2010), doi:10.1016/j.snb.2012.03.035

Highly formaldehyde-sensitive, transition-metal doped ZnO nanorods prepared by plasma-enhanced chemical vapor deposition

Peng Hu[1], Ning Han[1,2,*], Dangwen Zhang[1,3], Johnny C. Ho[2], and Yunfa Chen[1]

1. State Key Laboratory of Multi-Phase Complex Systems, Institute of Process Engineering, Chinese Academy of Sciences, Beijing 100190, P.R. China

2. Department of Physics and Materials Science, City University of Hong Kong, 83 Tat Chee Ave., H.K. SAR, China.

3. Graduate University of Chinese Academy of Sciences, Beijing 100049, P.R. China

[*] Corresponding author (Tel.: 86-10-82627057; fax: 86-10-62542803; E-mail address: nhan@home.ipe.ac.cn)

Abstract: One of the challenges in realizing metal oxide semiconductor gas sensors is to enhance the sensitivity of active materials in order to respond to the low concentration of detecting gases effectively and efficiently. In this report, transition metals such as Mn, Ni, Cu, and Co are used as dopants for the synthesis of highly formaldehyde-sensitive ZnO nanorods prepared by plasma enhanced chemical vapor deposition (PECVD) method. All the doped ZnO nanorods show improved formaldehyde-sensitivity as compared to undoped ZnO nanorods, and a gas sensitivity maximum of ~25 /ppm was obtained by using 10 mol% CdO activated 1.0 mol% Mn doped ZnO nanorods. Moreover, the ZnO nanorods have a higher sensitivity as compared to ZnO nanomaterials prepared by other methods such as precipitation and hydrothermal, which can be attributed to the abundant crystal defects induced by the dopants in a short crystallization process in this PECVD method.

Keywords: plasma-enhanced chemical vapor deposition; ZnO nanorods; transition metal dopants; formaldehyde gas sensors

1. Introduction

Zinc oxide (ZnO) is a versatile semiconductor material showing great potentials in piezoelectronics [1], solar energy harvesting [2], and gas sensors [3] etc., due to its abundance in earth and excellent electronic and optic properties. Since the first gas sensor reported by Seiyama *et al.* [4], ZnO based gas sensing elements have been one of the research focuses for the wide applications ranging from environmental toxic gas detection to domestic safety explosives alarming [5, 6]. However, the sensitivity is always one of the bottlenecks impeding sensor applications, especially when the detecting gas (detectant) has an extremely low permissive concentration. For example, as one of the common carcinogenic volatile organic compounds (VOCs), formaldehyde is strictly confined in the indoor air to be less than 0.8 mg/m^3 (~0.6 ppm) in most countries worldwide. In this context, super sensitive gas sensing materials are being explored recently to sense these trace gases [7-10].

From gas sensing materials point of view, the morphology (e.g. diameter of nanoparticles) [11], stoichiometry (e.g. oxygen vacancy) [12] as well as composition (e.g. dopants) [13, 14] all have significant influences on their gas sensing properties, in which the role of stoichiometry is widely concerned nowadays. In our previous studies, we proposed and verified a counter-intuitive sensing mechanism that high gas sensing property is expected when there are more donors than acceptors in ZnO nanoparticles prepared by the precipitation method [15] and ZnO nanorods with different aspect ratios prepared by the plasma-enhanced chemical vapor deposition (PECVD) method [16]. And recently, Chen *et al.* [17] also proved the dependence of

NO_2 gas sensing property of ZnO nanoflakes on the crystal defects. All these results highlight the effect of crystal defects in ZnO materials on the corresponding gas sensing properties.

Doping by other elements has long been verified to be an effective way to tailor the concentration of donors and acceptors in semiconductors, which is widely used to improve the gas sensing property of metal oxide semiconductors. For example, Sn-doped ZnO material showed a higher sensitivity than pure ZnO prepared by both precipitation and hydrothermal methods [9, 10, 18, 19]. However, it should also be noted that crystal defects are highly dependent on the preparation method of materials. For example, ZnO precursors would typically undergo a fast evaporation and recrystallization process in PECVD method, and thus more crystal defects are produced due to the incomplete crystallization. In contrast, in hydrothermal and precipitation processes, ZnO precursors undergo a long duration of high temperature crystallization, which minimizes crystal defects and thus decreases the gas sensing property. In our previous reports, ZnO nanorods prepared by PECVD method showed a higher sensitivity to formaldehyde than ZnO nanoparticles prepared by hydrothermal and precipitation methods [15, 16, 18].

Consequently, aiming at introducing more crystal defects into ZnO crystals to further improve the sensitivity, we combined doping method by transition-metal (Cu, Co, Ni, Mn) and preparation method by PECVD method in this report, and higher formaldehyde sensing ZnO nanorods were obtained accordingly.

2. Experimental

2.1 ZnO nanorods preparation

The transition metal doped ZnO nanorods prepared are similar to the thermal plasma synthesis method as we reported earlier [20]. Briefly, zinc powders and metal chlorides were mixed together as starting materials and feed into the plasma by a carrier gas. Oxygen was then introduced into the Argon plasma (30 kW, 4 MHz) together with the sheath gas to react with the starting materials. After the vaporization, reaction and crystallization process, the transition metal doped ZnO nanorods were obtained at the bottom of the collector. Transition metals such as Cu, Co, Ni, and Mn were adopted as the dopant, with the precursors of $CuCl_2$, $CoCl_2$, $NiCl_2$ and $MnCl_2$ at the required concentrations.

2.2 Characterization

The morphology and composition were characterized by a scanning electron microscope (SEM, JEOL JSM-6700F, Japan, 5 kV, 10 μA) and energy dispersive spectra (EDS) and a transmission electron microscope (TEM, HITACH–600A, Japan). The crystal phases were identified using X-ray diffraction (XRD, Panalytical X'pert Pro, the Netherlands, Cu-Kα1 radiation of λ = 0.15406 nm, 40 kV, 30 mA). The Raman spectra were measured on Horiba Jobin Yvon LabRAM HR800 Raman Microscope (514 nm Ar laser, 20 mW, France). And the PL spectra were recorded from 350 nm to 600 nm at room temperature by a 325 nm excitation from Xe lamp (Perkin Elmer LS 55 fluorometer).

The formaldehyde gas sensing properties of ZnO-based nanorods were examined

by using a home made instrument (see Supporting Information, Figure S1) as we reported earlier [21, 22]. Briefly, ZnO nanorods were ultrasonically dispersed in ethanol, and then drop-coated on a quartz sheet with two Pt wires connected on both ends using Ag paste (Wuhan Shuangjian Inc., China) to form a sensor prototype. The sensor was placed in a tube furnace to provide the work temperature. Formaldehyde was introduced into the quartz tube by bubbling its aqueous solution (0, 0.02, 1, 5, 10 wt%) using air (600 ml min^{-1}), whose concentration in gaseous phase was detected (Chinese standard GB/T 15516-1995) to be 0, 1, 32, 85, 205 ppm and the relative humidity (RH) was monitored by a humidity sensor to be 70 ± 10% at 25 ^{o}C. The bias on the sensor was set to 5 V and the current was recorded using Keithley 2601 Source-meter (Keithley Instrument Inc., the USA). The gas response is defined as the ratio of sensor resistance in air and in detectant (R_a/R_g), and sensitivity is defined as the ratio of response and corresponding concentration (response/ppm).

3. Results and Discussion

3.1 Preparation of Mn-doped ZnO nanorods

Figure 1 shows the morphology change of ZnO nanorods with different Mn doping concentrations ranging from 0.25 mol% to 4.0 mol%. It is obvious that the length of ZnO nanorods decreases a lot as the Mn doping concentration increases as observed by SEM and TEM in **Figure 1 (a)-(e)**. The typical lengths of Mn-doped ZnO nanorods are observed by TEM as shown in Figure 1 (a)-(e) inserts, and the axial growth rates are calculated as shown in Figure 1(f) based on the length and the residing time of the precursors in the plasma chamber. It is obvious that the growth

rate was greatly depressed by the high Mn doping concentrations. Compared to the pure ZnO nanorods (mean length of ~2 μm) as reported earlier [16], even the small doping concentration of 0.25 mol% Mn would make the nanorods shorter (mean length ~1.5 μm). All these show the suppression effect of Mn dopants on the axial growth of ZnO crystals. Mn prefers the tetragonal coordination with tetragonal or cubic structure in oxides (e.g. PDF 01-0799 and 01-1061), while the ZnO crystal is tetragonal coordinated with hexagonal structure (PDF 01–089–0511); therefore, if Mn is doped into the ZnO crystal, an extra energy should be provided and the ZnO lattice is then distorted a bit. It is also noted that although all the XRD patterns of Mn-doped ZnO nanorods show the wurtzite structural peaks as shown in **Figure 2 (a)**, the peak at ~34.5^{o} (corresponding to (002) plane) is shifted accordingly with the Mn dopant concentration as shown in **Figure 2 (b)**. According to the Bragg's law, a Mn doping concentration of 2.0 mol% (the concentration was also verified by EDS results) would increase the plane spacing of ZnO (002) plane by 0.002 nm. Moreover, Mn-O related Raman shifts at ~529 and 573 cm^{-1} also begin to appear at a low Mn doping concentration of 0.25 mol% as shown in **Figure 3** as compared with the Raman shift of pure ZnO ($3E_{2L}$ vibration mode at ~329 cm^{-1} and E_{2H} mode at ~438 cm^{-1}) [23, 24]. Consequently, all these results proved the successful doping of Mn into the ZnO crystal with different concentrations.

3.2 Gas sensing property of Mn-doped ZnO nanorod

The gas sensing property of Mn-doped ZnO nanorods are measured by using formaldehyde as a probe at 300 and 400 ^{o}C, where gas sensing maxima are obtained

for ZnO related materials, as shown in **Figure 4**. From **Figure 4(a)**, it is obvious that 1.0 mol% Mn-doped nanorods have the highest formaldehyde gas sensing property at both 300 and 400 ^{o}C, with a maximum response of 92 to 32 ppm formaldehyde at 300 ^{o}C. From the response and recovery curves in **Figure 4(b)**, the response and recovery time (defined as the times needed for the signal to arrive at 90% and get back to 10% of the full response) are estimated to be in the order of seconds considering 1-2 min is needed for the saturation of formaldehyde gas near the sensor (for details see Supporting Information Figure S1 and S2). Furthermore, a linear response of the 1.0 mol% Mn-doped ZnO to different concentrations of formaldehyde is also attained as shown in the calibration curve in **Figure 4(c)**. Then the sensitivity (defined as response/ppm) can be estimated to be as high as ~2.9/ppm.

It is reported CdO particles can activated In_2O_3 materials to further increase the gas sensing property [7, 8], and we also reported a highly sensitive, selective and stable CdO activated Sn-doped ZnO material based formaldehyde gas sensor [10]. Then in this study, we used CdO (10 mol%) to activate the 1.0 mol% Mn-doped ZnO nanorods (by dipping the doped ZnO nanorods into $Cd(NO_3)_2$ aqueous solution and then calcination) for the higher sensitivity. The sensitivity of the above-mentioned CdO activated Sn-doped ZnO nanoparticles by co-precipitation method and Mn-doped ZnO nanorods by PECVD method are compared in **Figure 5**. A far higher sensitivity of ~25 /ppm was yielded for the 1.0 mol% Mn-doped ZnO nanorods as compared to the sensitivity of 10 /ppm for the 2.2 mol% Sn-doped ZnO nanoparticles [10]. This would give a 1.5X response to the permissive formaldehyde concentration

of 0.6 ppm in indoor air standard, which is appealing in the real applications. Moreover, the response and recovery time of CdO activated Mn-doped ZnO nanorods are far shorter than those of CdO activated Sn-doped ZnO nanoparticles. CdO is also an n-type semiconductor (Eg~2.3 eV), and there is believed to be excess Cd in the surface layer of CdO [25]. The excess Cd might be the key to favoring oxygen adsorption in gas sensing process of ZnO.

Ni, Cu, Co were also adopted as dopants (0.5 mol%) in the ZnO nanorod growth with SEM images shown in **Figure 6 (a)-(c)**. All samples show the nanorod-shape morphology, although the Cu-doped ZnO nanorods have a much larger length and forms clusters as shown in **Figure 6 (b)**. The doped ZnO crystals are all in wurtzite phase as shown in the XRD pattern in **Figure 6 (d)**. The formaldehyde gas sensing properties of the Ni, Cu, Co doped ZnO nanorods are tested as shown in **Figure 7**. For comparison, we also prepared Sn-doped ZnO nanorods by PECVD, and plotted the responses of pure ZnO nanorods and Sn-doped ZnO nanorods together. It is obvious that doped ZnO have much higher response than the undoped one, and Co, Ni, Sn doped ones have a nearly 4-fold increase in the response.

The formaldehyde gas sensitivity is compared regarding pure and different metal doped ZnO nanorods and nanoparticles prepared by PECVD, co-precipitation and hydrothermal methods, as shown in **Table 1**. A general conclusion can be found that sensitivity of ZnO material can be improved by doping by proper metals, e.g. Sn dopant in all the three preparation methods. More importantly, the pure and doped ZnO nanorods prepared by PECVD method all have a far higher sensitivity as

compared with their counterparts in both precipitation and hydrothermal methods. For example, pure ZnO nanoparticles and nanorods prepared by precipitation and hydrothermal methods only have a sensitivity of 0.1-0.3/ppm, which is far lower than that of pure ZnO nanorods (~0.6/ppm) prepared by PECVD. Although Mn-doped ZnO material shows a decreased sensitivity as prepared in precipitation method (~0.1/ppm), it has a far higher sensitivity if prepared by PECVD methods (~2.9/ppm). All these results show the superiority of PECVD method in preparing highly sensitive ZnO materials.

In our previous study, we proposed a counter-intuitive sensing mechanism that gas sensing property is highly dependent on the crystal defects in ZnO crystals. High sensitivity is preferred by a higher content of donor related defects and a lower content of acceptor related defects [15], because the donors would provide electrons for the adsorbed oxygen to produce the active ion-sorbed oxygen as shown in Equations (1) (3) and (4) (D is donor). On the other hand, acceptors would be recombined with electrons as shown in Equation (2) (A is acceptor), preventing adsorbed oxygen to form the active ion-sorbed oxygen. Therefore, more formaldehyde would be oxidized to arise higher response if there are more donors and less acceptors in ZnO crystals. And recently, there are more similar proofs regarding the role of crystal defects in gas sensing materials [17, 28].

$$D \rightarrow D^{+} + e^{-} \quad (1)$$

$$A + e^{-} \rightarrow A^{-} \quad (2)$$

$$O_2 + 2\,e^{-} \rightarrow 2\,O_{ad}^{-} \quad (3)$$

$$HCHO + 2\ O_{ad}^{-} \rightarrow H_2O + CO_2 + 2\ e^{-} \quad (4)$$

To probe the crystal defects in doped ZnO material, PL spectra were recorded using 325 nm Xe lamp excitation, with normalized spectra shown in **Figure 8**. ZnO has a bandgap of ~3.3 eV (375 nm), which takes a small part in the PL spectra in **Figure 8**. On the contrary, the luminescence emission from crystal defects (>390nm) dominates the entire spectra. Moreover, it is noted in **Figure 8** that the relative intensity of the luminescence from crystal defects is higher for the transition metal doped ZnO material as compared with that of the pure ZnO. Therefore, more crystal defects would be expected for the doped ZnO material. We previously used Gaussian decomposition to quantitatively study the content of crystal defects in pure ZnO crystal [15, 16]. However, this method can not be used for doped ZnO material directly as more information are needed from solid state physics studies, such as: (1) how many kinds of luminescence are originated from the dopants and/or from crystal defects and (2) where are they located in the spectra.

Considering the preparation methods, it is well known that precursors undergo a high speed evaporation and condensation process (in the order of sub second) in PECVD method, while precursors suffer a long duration (hours and even days) of high temperature and high pressure process in hydrothermal method. Consequently, precursors form high-quality crystals in hydrothermal process, while more defects would be formed in PECVD method due to the incomplete crystallization. Therefore, ZnO sensing material prepared by PECVD method shows a far higher sensing property than that prepared by precipitation and hydrothermal methods, which

demonstrates the potency of PECVD method in the gas sensing material preparation.

4. Conclusions

Transition metals including Mn, Ni, Cu, and Co doped ZnO nanorods are prepared by plasma enhanced chemical vapor deposition method (PECVD). The doped ZnO nanorods show the superior formaldehyde-sensing property, with a sensing maximum of ~25/ppm for 10 mol% CdO activated 1.0 mol% Mn doped ZnO nanorods in a few seconds response and recovery time. The sensitivity and response/recovery time are advantageous as compared with ZnO based sensing materials prepared by precipitation and hydrothermal methods, due to the abundant crystal defects in the fast crystallization process in PECVD.

Acknowledgement

The authors thank National 863 Program (no. 2007AA061401) for the support.

References

[1] Z. Wang and J. Song, Piezoelectric nanogenerators based on zinc oxide nanowire arrays, Science 312 (2006) 242-246.

[2] M. Law, L. E. Greene, J. C. Johnson, R. Saykally and P. D. Yang, Nanowire dye-sensitized solar cells, Nat. Mater. 4 (2005) 455-459.

[3] Z. Fan, D. Wang, P. Chang, W. Tseng and J. Lu, ZnO nanowire field-effect transistor and oxygen sensing property, Appl. Phys. Lett. 85 (2004) 5923.

[4] T. Seiyama, A. Kato, K. Fujiishi and M. Nagatani, A new detector for gaseous components using semiconductive thin films, Anal. Chem. 34 (1962) 1502-1503.

[5] Z. Liu, T. Fan, D. Zhang, X. Gong and J. Xu, Hierarchically porous ZnO with high sensitivity and selectivity to H_2S derived from biotemplates, Sens. Actuators B 136 (2009) 499-509.

[6] O. Lupan, V. V. Ursaki, G. Chai, L. Chow, G. A. Emelchenko, I. M. Tiginyanu, A. N. Gruzintsev and A. N. Redkin, Selective hydrogen gas nanosensor using individual ZnO nanowire with fast response at room temperature, Sens. Actuators B 144 (2010) 56-66.

[7] T. Chen, Z. Zhou and Y. Wang, Effects of calcining temperature on the phase structure and the formaldehyde gas sensing properties of CdO-mixed In_2O_3, Sens. Actuators B 135 (2008) 219-223.

[8] T. Chen, Q. J. Liu, Z. L. Zhou and Y. D. Wang, The fabrication and gas-sensing characteristics of the formaldehyde gas sensors with high sensitivity, Sens. Actuators B 131 (2008) 301-305.

[9] J. Xu, X. Jia, X. Lou, G. Xi, J. Han and Q. Gao, Selective detection of HCHO gas using mixed oxides of ZnO/$ZnSnO_3$, Sens. Actuators B 120 (2007) 694-699.

[10] N. Han, X. F. Wu, D. W. Zhang, G. L. Shen, H. D. Liu and Y. F. Chen, CdO activated Sn-doped ZnO for highly sensitive, selective and stable formaldehyde sensor, Sens. Actuators B 152 (2011) 324-329.

[11] C. Xu, J. Tamaki, N. Miura and N. Yamazoe, Grain size effects on gas sensitivity of porous SnO_2-based elements, Sens. Actuators B 3 (1991) 147-155.

[12] Y. Zhang, J. Q. Xu, Q. Xiang, H. Li, Q. Y. Pan and P. C. Xu, Brush-like hierarchical ZnO nanostructures: synthesis, photoluminescence and gas sensor properties, J. Phys. Chem. C 113 (2009) 3430-3435.

[13] G. Korotcenkov, Gas response control through structural and chemical modification of metal oxide films: state of the art and approaches, Sens. Actuators B 107 (2005) 209-232.

[14] N. Barsan, D. Koziej and U. Weimar, Metal oxide-based gas sensor research: How to?, Sens. Actuators B 121 (2007) 18-35.

[15] N. Han, X. F. Wu, L. Y. Chai, H. D. Liu and Y. F. Chen, Counterintuitive sensing mechanism of ZnO nanoparticle based gas sensors, Sens. Actuators B 150 (2010) 230-238.

[16] N. Han, P. Hu, A. H. Zuo, D. W. Zhang, Y. J. Tian and Y. F. Chen, Photoluminescence investigation on the gas sensing property of ZnO nanorods prepared by plasma-enhanced CVD method, Sens. Actuators B 145 (2010) 114-119.

[17] M. Chen, Z. Wang, D. Han, F. Gu and G. Guo, Porous ZnO polygonalnanoflakes:

synthesis, use in high-sensitivity NO_2 gas sensor, and proposed mechanism of gas sensing, J. Phys. Chem. C 115 (2011) 12763-12773.

[18] N. Han, L. Chai, Q. Wang, Y. Tian, P. Deng and Y. Chen, Evaluating the doping effect of Fe, Ti and Sn on gas sensing property of ZnO, Sens. Actuators B 147 (2010) 525-530.

[19] N. Han, H. D. Liu, X. F. Wu, D. Y. Li, L. Y. Chai and Y. F. Chen, Pure and Sn-, Ga- and Mn-doped ZnO gas sensors working at different temperatures for formaldehyde, humidity, NH_3, toluene and CO, Appl. Phys. a-Mater. 104 (2011) 627-633.

[20] P. Hu, F. L. Yuan, L. Y. Bai, J. L. Li and Y. F. Chen, Plasma synthesis of large quantities of zinc oxide nanorods, J. Phys. Chem. C 111 (2007) 194-200.

[21] N. Han, Y. J. Tian, L. Q. Wei, C. Wang and Y. F. Chen, NiO thin film fabricated by electrophoretic deposition and formaldehyde gas sensing property thereof, J. Nanosci. Nanotechnol. 9 (2009) 1346-1349.

[22] N. Han, Y. J. Tian, X. F. Wu and Y. F. Chen, Improving humidity selectivity in formaldehyde gas sensing by a two-sensor array made of Ga-doped ZnO, Sens. Actuators B 138 (2009) 228-235.

[23] T. C. Damen, S. P. S. Porto and B. Tell, Raman effect in zinc oxide, Phys. Rev. 142 (1966) 570-574.

[24] C. Bundesmann, N. Ashkenov, M. Schubert, D. Spemann, T. Butz, E. M. Kaidashev, M. Lorenz and M. Grundmann, Raman scattering in ZnO thin films doped with Fe, Sb, Al, Ga, and Li, Appl. Phys. Lett. 83 (2003) 1974-1976.

[25] R. M. Gabr, M. M. Girgis and A. M. El-Awad, Role of CdO/Cd^{2+} content on the electrical conductivity and catalytic behaviour of $Co_{1.0-x}$-Cd_x-$Fe_{2.0}$ oxide/spinel system ($0.0 < x < 0.5$) for the decomposition of 2 propanol, Mater. Chem. Phys. 28 (1991) 413-429.

[26] J. Xu, Y. Chen, D. Chen and J. Shen, Hydrothermal synthesis and gas sensing characters of ZnO nanorods, Sens. Actuators B 113 (2006) 526-531.

[27] L. Zhang, J. Zhao, J. Zheng, L. Li and Z. Zhu, Shuttle-like ZnO nano/microrods: Facile synthesis, optical characterization and high formaldehyde sensing properties, Appl. Surf. Sci. 258 (2011) 711-718.

Biographies

Peng Hu received his PhD in Chemical Engineering in Institute of Process Engineering, Chinese Academy of Sciences, P.R. China in 2008, and now he is an assistant professor of the Institute of Process Engineering. His current research fields focus on the synthesis, characterization and self-assembly of inorganic nanoparticles with novel structures, such as 1D nanostructures, hollow structures, and property investigation and functionalization of these novel nanostructures. Contact: pengh@home.ipe.ac.cn.

Ning Han received his PhD in 2010 in Chemical Engineering at Institute of Process Engineering, Chinese Academy of Sciences, and now is a research associate in City University of Hong Kong. His research interests are preparation and application of gas sensing materials and technologies to fabricate gas sensors and the gas sensing mechanism. And he is also interested in III-V compound semiconductors preparation and applications. Contact: cattleox0422@126.com.

Dangwen Zhang received her bachelor's degree in Chemical Engineering and Technology at Lanzhou Jiaotong University, GanSu province, China, in 2006. She is now a doctor candidate of Institute of Process Engineering, Chinese Academy of Sciences. She had committed herself to preparation of a variety of ZnO nano-structures such as nanobelts, nanorods and so on. Contact: dwzhang@home.ipe.ac.cn.

Johnny C. HO received his M.S. and Ph.D. in materials science and engineering from the University of California at Berkeley in 2005 and 2009, respectively. He is now an assistant professor in Department of Physics and Materials Sciences, City University of Hong Kong. He is leading a group concentrating on materials science, including nanophotonics, nanoelectronics, nanomaterial based energy harvesting and sensors and so on. Contact: johnnyho@cityu.edu.hk.

Yunfa Chen received his PhD in Material Science at Universit Louis Pasteur Strasbourg (ULP), France in 1993. He is a professor of the Graduate University of Chinese Academy of Sciences, and Research Professor and Vice Director of Institute of Process Engineering, Chinese Academy of Sciences. His current research interests are preparation and assembly of nanoparticles, functional materials, organic-inorganic composite materials and layered materials. And he is also interested in industrial applications of nanomaterials. Contact: yfchen@home.ipe.ac.cn.

Figure Captions

Figure 1. (a)-(e) are SEM and TEM (inserts) images of Mn-doped ZnO nanorods at different Mn doping concentrations of: (a) 0.25 mol%, (b) 0.5 mol%, (c) 1.0 mol%, (d) 2.0 mol% and (e) 4.0 mol%, and (f) is the axial growth rate of pure ZnO nanorod and Mn doped ZnO nanorods in (a)-(e).

Figure 2. (a) XRD patterns and (b) magnified peaks at ~34.5^{o} of pure ZnO and Mn-doped ZnO nanorods (the peak are Voigt fitted with a correlation coefficient of R^2>0.99).

Figure 3. Raman spectra of pure ZnO and 0.25 mol%, 0.5 mol%, 1.0 mol%, 2.0 mol% and 4.0 mol% Mn-doped ZnO nanorods.

Figure 4. Formaldehyde gas sensing property of Mn-doped ZnO nanorods: (a) Sensing property dependence on the Mn dopant concentrations, (b) response and recovery curves of 1.0 mol% Mn doped ZnO nanorod (0 ppm means RH 70%) and (c) linear relationship of response of 1.0 mol% Mn doped ZnO nanorod versus formaldehyde concentrations.

Figure 5. Formaldehyde response comparison of 10 mol% CdO activated 1.0 mol% Mn doped ZnO nanorods (CdO-MZO) at 300 ^{o}C, and 10 mol% CdO activated 2.2 mol% Sn-doped ZnO nanoparticles (CdO-SZO) at 200 ^{o}C (0 ppm means RH 70%).

Figure 6. SEM images of (a) Ni-doped (b) Cu-doped and (c) Co-doped ZnO nanorods (doping concentrations of 0.5 mol%), and (d) is the corresponding XRD patterns of (a)-(c).

Figure 7. Formaldehyde gas sensing properties of PECVD method prepared pure and

Cu, Co, Ni, Sn (0.5 mol%) doped ZnO nanorods.

Figure 8. Normalized PL spectra of pure ZnO and Mn, Co, Cu, Ni, Sn (0.5 mol%) doped ZnO nanorods.

Table 1. Formaldehyde gas sensing property comparison of ZnO and doped ZnO by different methods

Preparation method	Material	Sensitivity (response/ppm)	Ref.
PECVD	ZnO Nanorods	~0.6	[16]
	Mn-ZnO	~2.9	This study
	Sn-ZnO	~2.9	This study
Precipitation	ZnO nanoparticles	~0.28	[15]
	Sn-ZnO	~0.65	[10]
	Mn-ZnO	~0.1	[19]
Hydrothermal	ZnO nanoparticles	~0.2	[9,18]
	ZnO nanorods	~0.1	[12, 26]
	Sn-ZnO	~0.65	[18]

Figure1

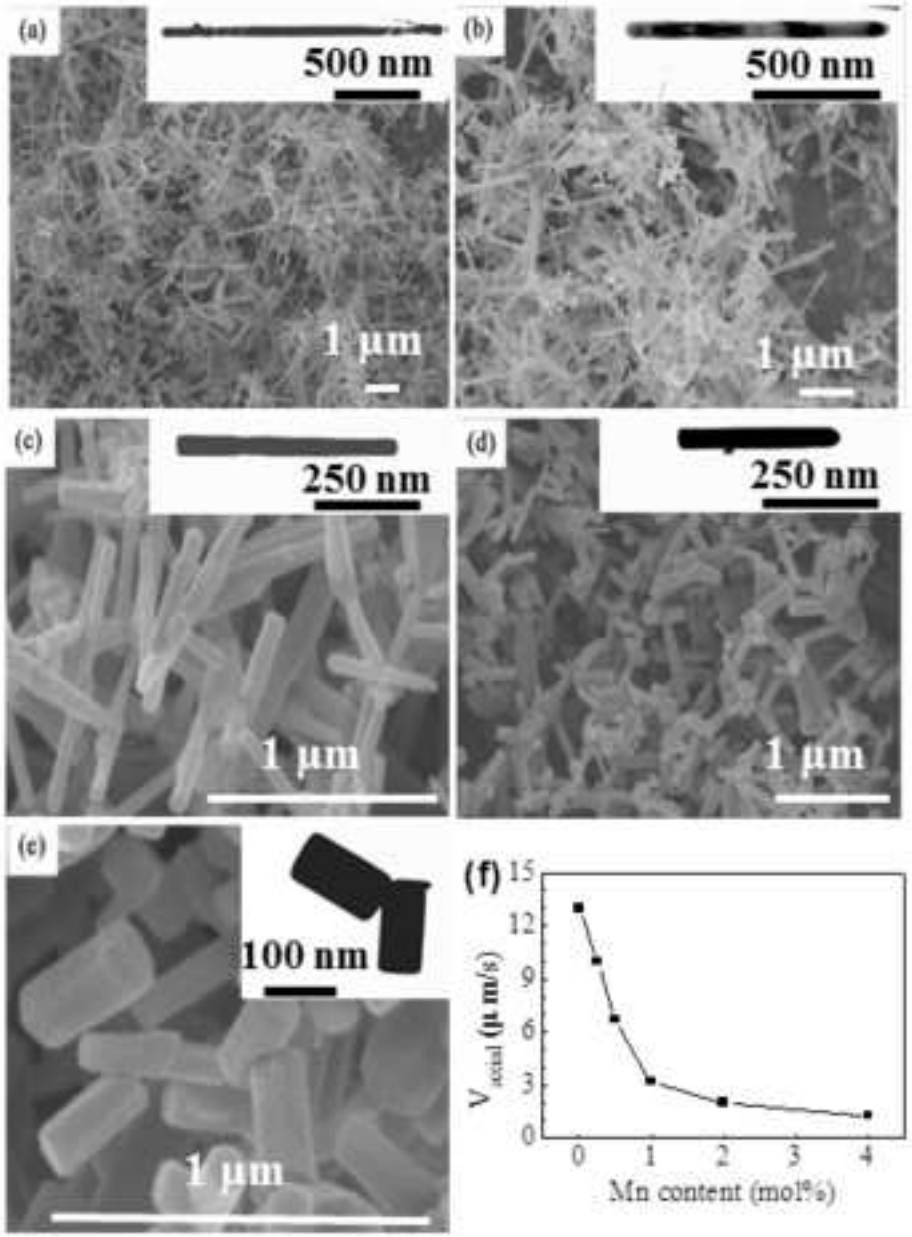
(a)
500 nm
1 μm
(b)
500 nm
1 μm
(c)
250 nm
1 μm
(d)
250 nm
1 μm
(e)
100 nm
1 μm
(f)
V_{axial} (μm/s)
Mn content (mol%)
0
3
6
9
12
15
0
1
2
3
4

Figure2

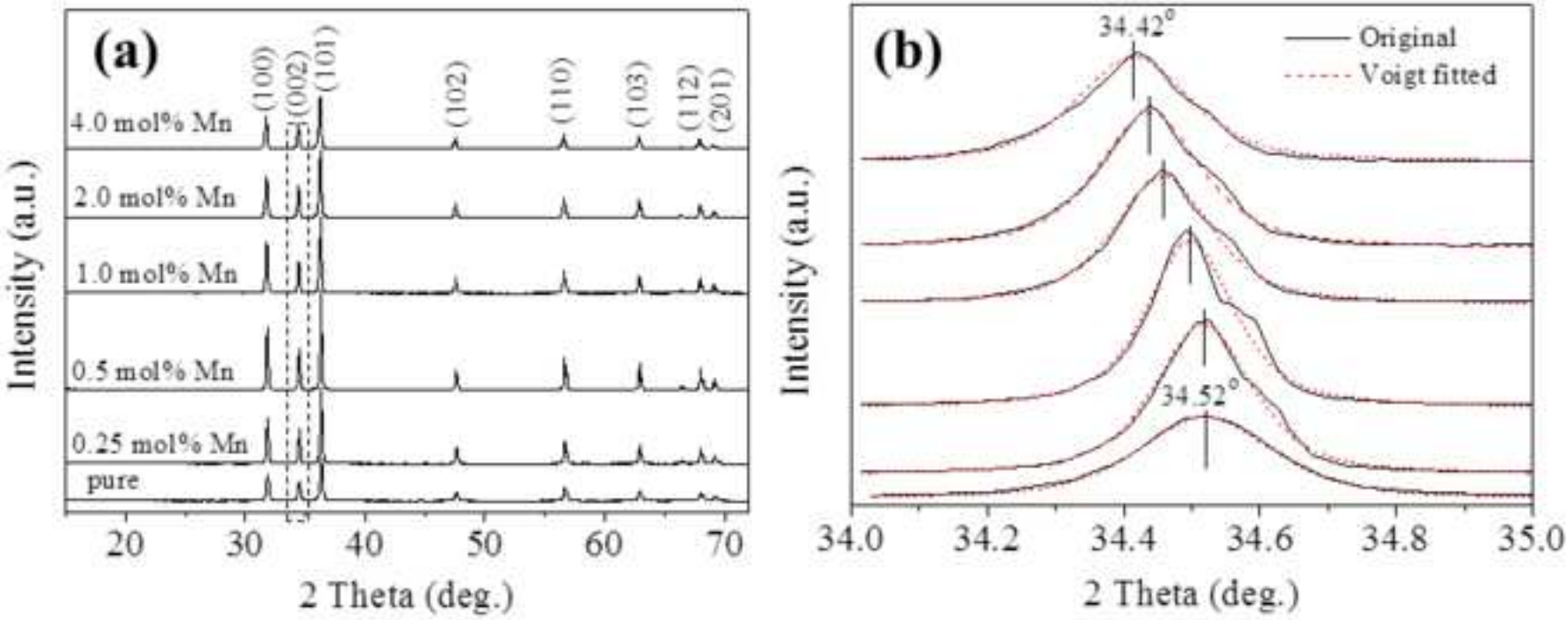
(a)
(100)
(002)
(101)
(102)
(110)
(103)
(112)
(201)
4.0 mol% Mn
2.0 mol% Mn
1.0 mol% Mn
0.5 mol% Mn
0.25 mol% Mn
pure
Intensity (a.u.)
20
30
40
50
60
70
2 Theta (deg.)
(b)
34.42°
34.52°
Original
Voigt fitted
Intensity (a.u.)
34.0
34.2
34.4
34.6
34.8
35.0
2 Theta (deg.)

Figure3

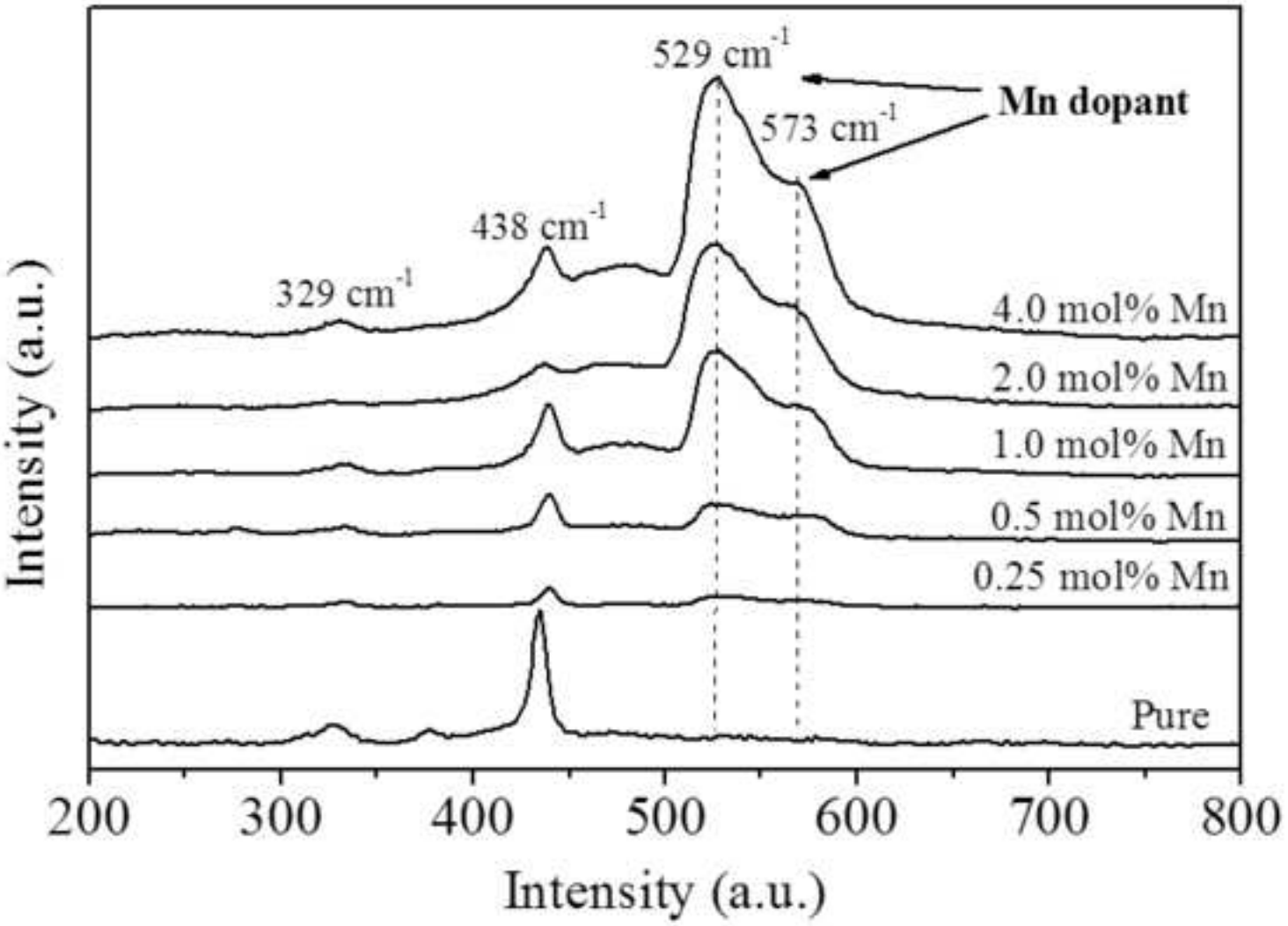
529 cm-1
Mn dopant
573 cm-1
438 cm-1
329 cm-1
4.0 mol% Mn
2.0 mol% Mn
1.0 mol% Mn
0.5 mol% Mn
0.25 mol% Mn
Pure
Intensity (a.u.)
200
300
400
500
600
700
800
Intensity (a.u.)

Figure4

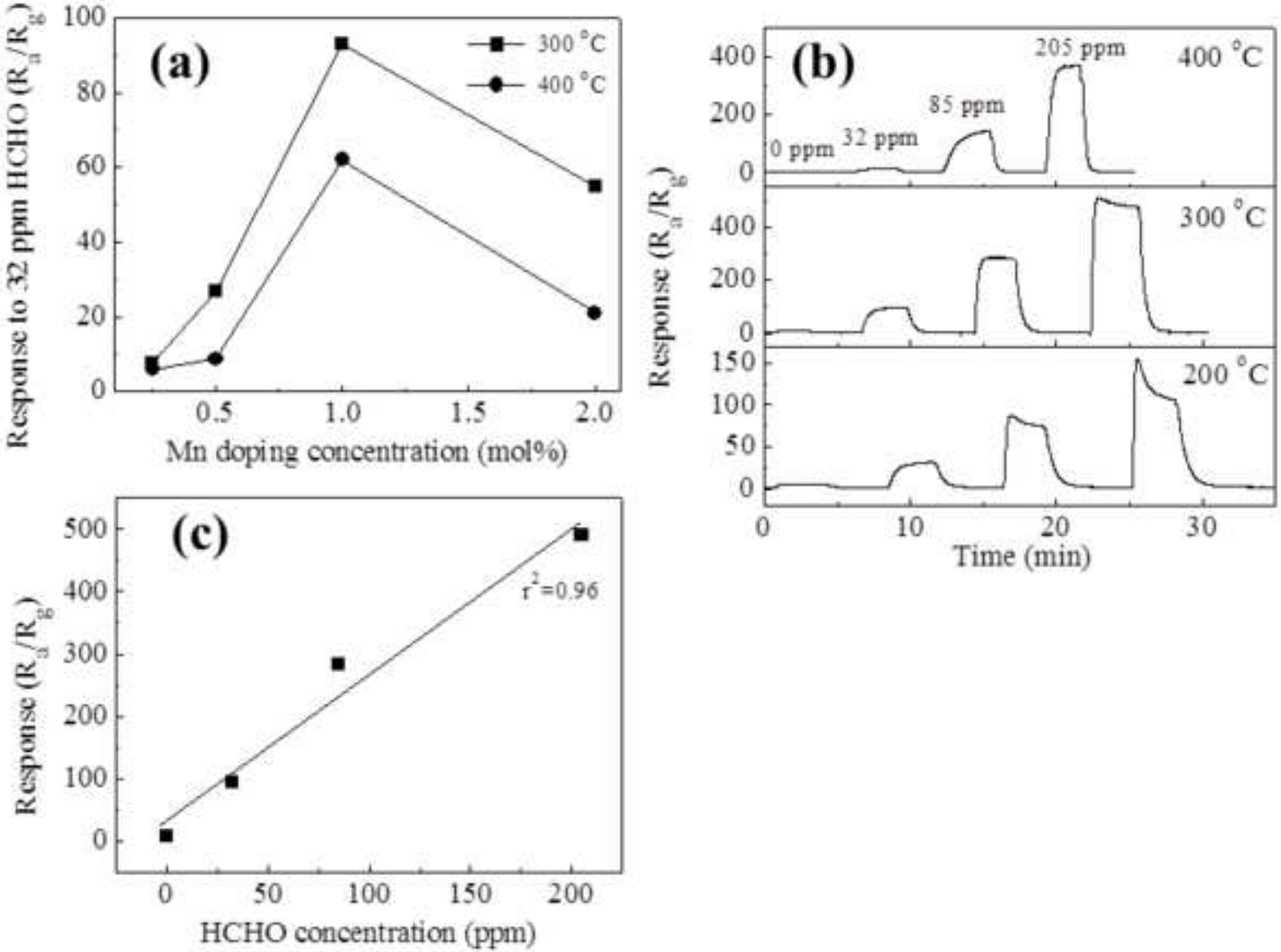
(a)
300 °C
400 °C
Response to 32 ppm HCHO (R_a/R_g)
Mn doping concentration (mol%)
(b)
205 ppm
400 °C
85 ppm
32 ppm
0 ppm
300 °C
200 °C
Response (R_a/R_g)
Time (min)
(c)
r^2=0.96
Response (R_a/R_g)
HCHO concentration (ppm)

Figure5

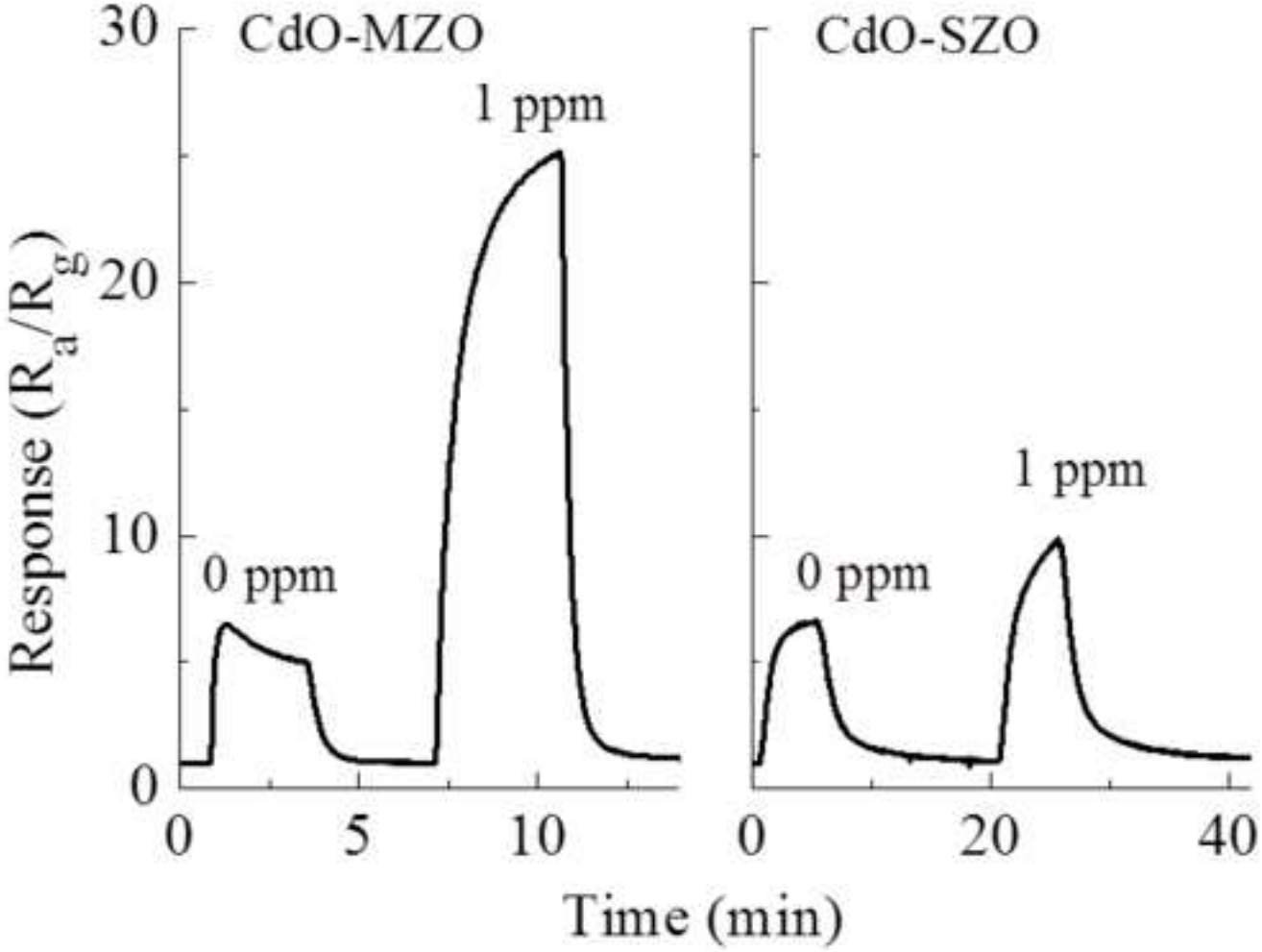
CdO-MZO
CdO-SZO
1 ppm
1 ppm
0 ppm
0 ppm
Response (R_a/R_g)
Time (min)
0
10
20
30
0
5
10
0
20
40

Figure6

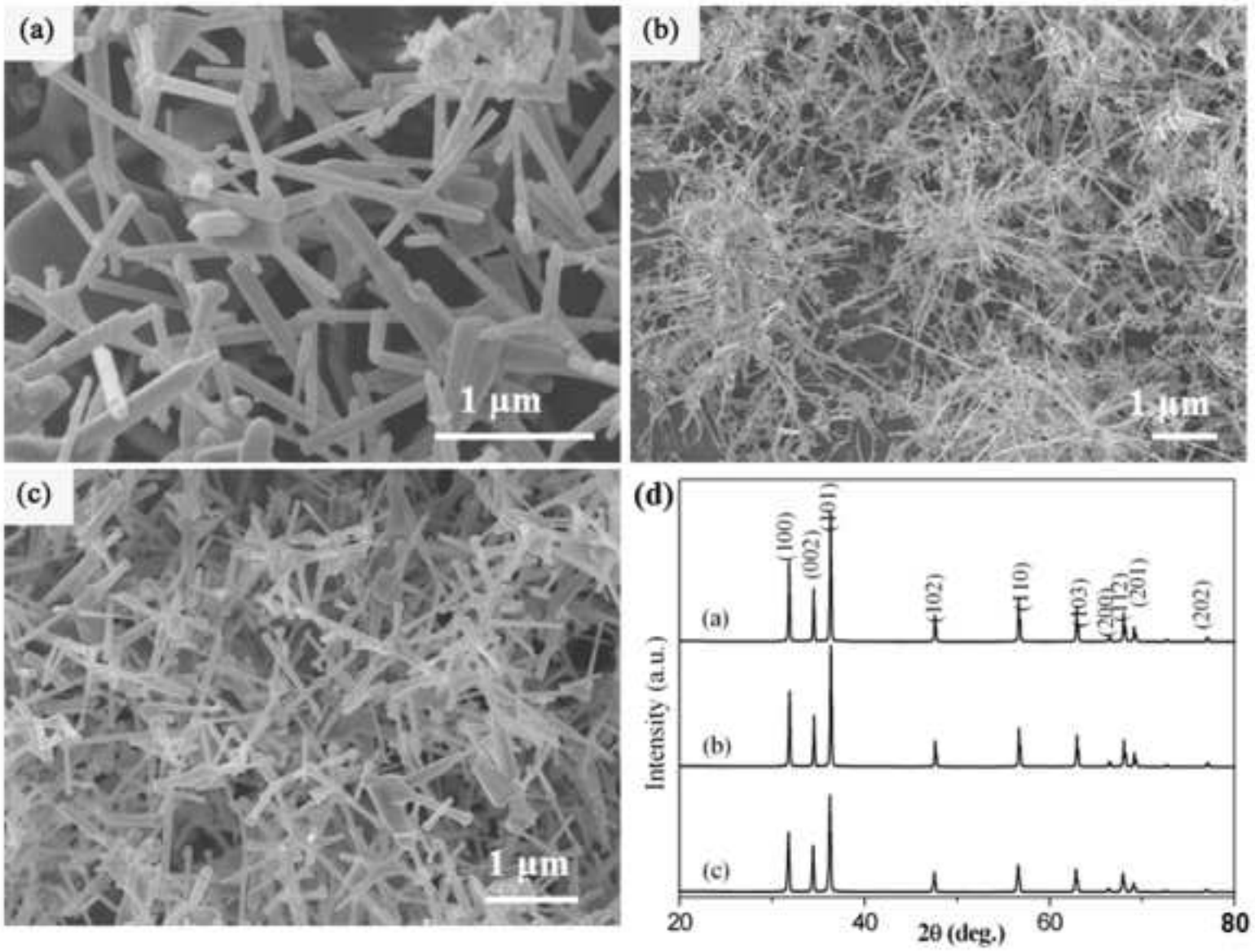
(a)
1 μm
(b)
1 μm
(c)
1 μm
(d)
(100)
(002)
(101)
(102)
(110)
(103)
(200)
(112)
(201)
(202)
(a)
(b)
(c)
Intensity (a.u.)
20
40
60
80
2θ (deg.)

Figure7

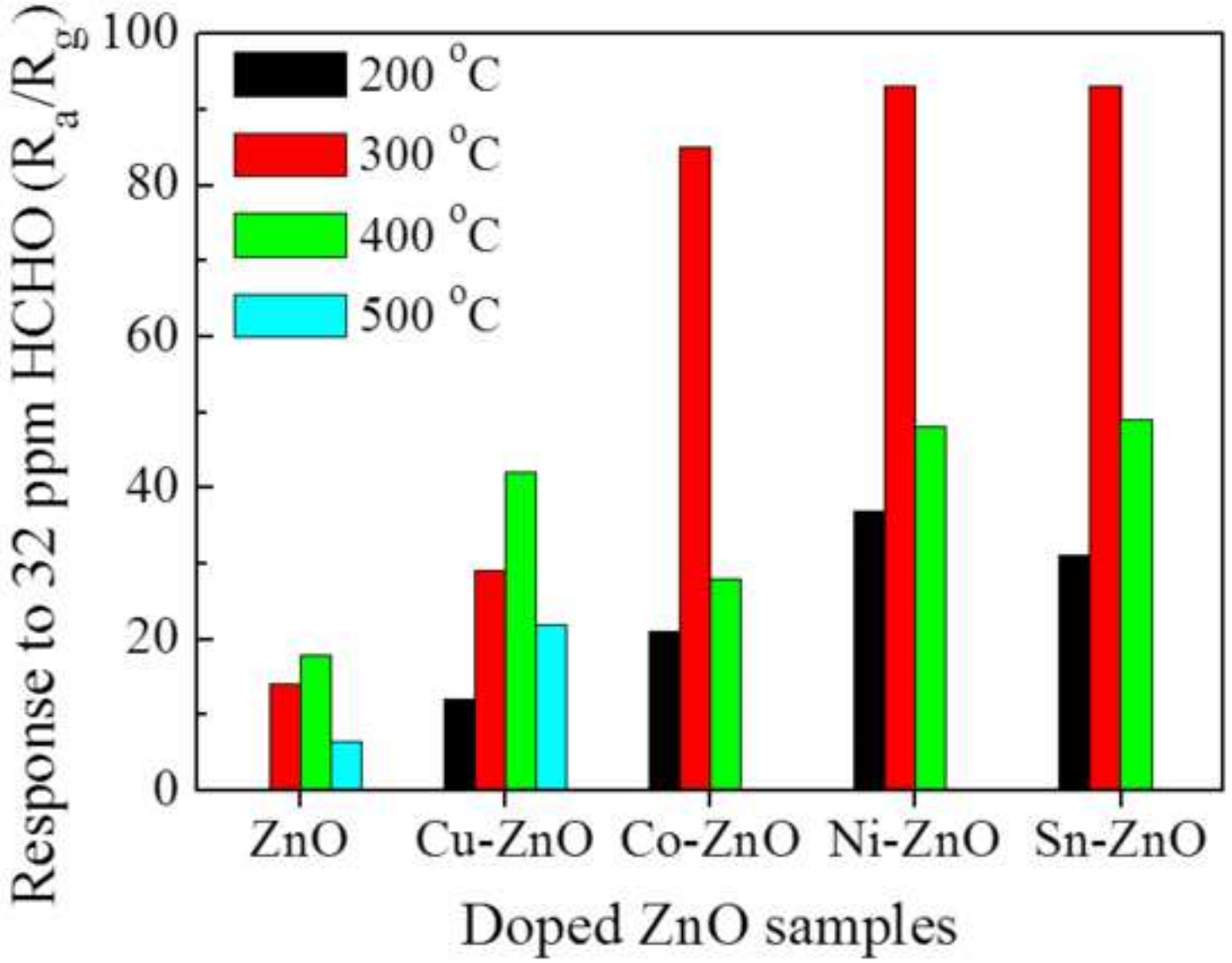
Response to 32 ppm HCHO (R_a/R_g)
100
80
60
40
20
0
200 °C
300 °C
400 °C
500 °C
ZnO
Cu-ZnO
Co-ZnO
Ni-ZnO
Sn-ZnO
Doped ZnO samples

Figure8

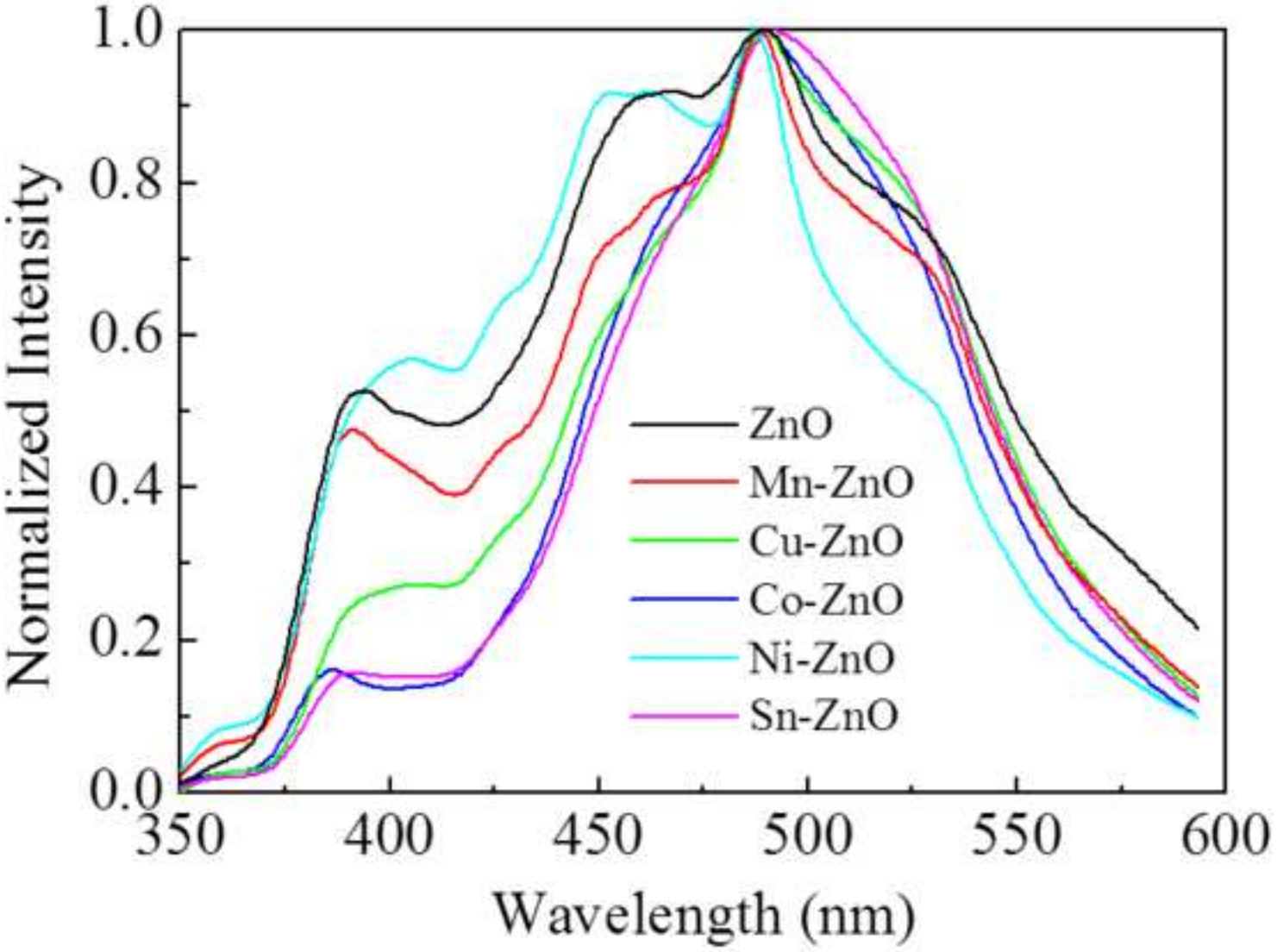
Normalized Intensity
1.0
0.8
0.6
0.4
0.2
0.0
350
400
450
500
550
600
Wavelength (nm)
ZnO
Mn-ZnO
Cu-ZnO
Co-ZnO
Ni-ZnO
Sn-ZnO